Scholars LITERATURE

La Prensa Medica Argentina

Research Article

Volume 105 Issue 6

Diagnosis of Patients with Hypothyroidism Using Spectrochemical Analysis of Blood Sera

Al-Zubaidi MA[1]*, Salman AMH[1], Mohsin RA[2] and Abdul Khaleq MA[3]

[1]Department of Clinical Laboratory Sciences, College of Pharmacy, Mustansiriyah University, Baghdad, Iraq
[2]Department of Pharmacology and Toxicology, College of Pharmacy, Mustansiriyah University, Baghdad, Iraq
[3]Department of Dentistry, Al-Rasheed University College, Baghdad, Iraq

Abstract

Biochemical tests are critical in the management of patients with hypothyroidism (HT). Fourier Transfer Infrared (FTIR) which allows for global bio-fluid metabolic profiling may give more appropriate information by measuring a broad range of metabolic parameters in bio-fluid. Here we present the application of FTIR with chemo metric analysis for the diagnosis of patients with hypothyroidism (HT). Twenty-six patients and twenty-six healthy sex-matched individuals were prospectively recruited in this study. FTIR spectra were measured in serum samples. The most informative variables obtained by FTIR were selected by variable importance in the projection (VIP) value after creating an OPLS-DA model at three specific regions: 900-1200 cm^{-1}, 1500-1700 cm^{-1}, and 2800-3100 cm^{-1}. The significance of each created model was validated by P-value ($P<0.05$) of CV-ANOVA. Multivariate analysis (OPLS-DA) of the FTIR data revealed the differences in the serum metabolic components of patients with hypothyroidism. OPLS-DA models revealed validation for 900-1200 cm^{-1} region (R2Y(cum)=0.934; Q2(cum)=0.514), 1500-1700 cm^{-1} region (R2Y(cum)=0.726; Q2(cum)=0.555), and 2800-3100 cm^{-1} region (R2Y(cum)= 0.959; Q2(cum)= 0.618) with P-value <0.05 of CV-ANOVA. The results indicated that FTIR spectral biomarkers distinguish the serum of patients with hypothyroidism, for example, carbohydrates and nucleic acids, proteins (Amide I/ Amide II), and lipids biomolecules.

In summary, this work demonstrates that FTIR spectroscopy supported by Orthogonal Partial Least Squares Discriminant Analysis (OPLS-DA) has the potential to become a fast and reagent-free method for biochemical characterization of serum that consequently could have a diagnostic significance in patients with hypothyroidism (HT).

Keywords: Blood serum analysis; Chemo metric analysis; FTIR spectroscopy; Hypothyroidism

Correspondence to: Mohammed A Al-Zubaidi, Department of Clinical Laboratory Sciences, College of Pharmacy, Mustansiriyah University, Baghdad, Iraq; E-mail: mohmsc82@gmail.com

Citation: Al-Zubaidi MA, Salman AMH, Mohsin RA, et al. (2019) Diagnosis of Patients with Hypothyroidism Using Spectrochemical Analysis of Blood Sera. Prensa Med Argent, Volume 105:6. 250

Received: November 22, 2019; **Accepted:** December 09, 2019; **Published:** December 14, 2019

Introduction

Thyroid hormones including both thyroxin (T4) and triiodothyronine (T3) are important for normal development and proper function of virtually all organs [1]. They modulate the metabolism of carbohydrate and lipid, as well as stimulate protein synthesis [2-4]. The synthesis and release of these hormones by the most important glands, known thyroid gland, are controlled by the anterior pituitary thyroid stimulating hormone (TSH) which is synthesized in response to hypothalamic TSH-releasing hormones [5]. Abnormal in the function of the thyroid gland is medically known thyroid disease; both hypothyroidism (low amount of thyroid hormones) and hyperthyroidism (high amount of thyroid hormones) are the major conditions that involved the thyroid gland [6]. Vibrational spectroscopic techniques, including infrared absorption, have developed across the previous twenty years as introducing routine analytical techniques for a large variety of applications, as they providing particular biochemical information and molecular structure of analyzed samples without the use of extrinsic stable labels [7,8]. Vibrational spectroscopy approach has some advantage as it is a technique of a reagent-free testing method and gives allowance for a rapid and non-destructive diagnosis as compare with traditional problems associated with serum/ plasma in diagnosis and screening. This method is comparatively easy, reproducible, require minimum preparation of sample as well as small amount of sample requirements [9,10]. The FTIR technique relies on the distinctive absorbance of corresponding molecular vibration in the functional group of biomolecules such as lipids, amino acids, proteins, carbohydrates, as well as chemical bonds between two atoms. The fundamental concept of FTIR is when these biochemical compounds are subjected to infrared radiation, the radiant energy corresponds to the energy of a particular molecular vibration and absorption happens. FTIR can offer assistant to recognize unknown materials, determine a sample's quality or consistency, and define the number of components in combination samples [8]. Numerous spectroscopic studies show the potential of FTIR spectroscopy for medical diagnosis, commonly from tissue [11] and recently from fluids such as serum [12-14], plasma [15,16] and tears [17]. Despite its potential, FTIR spectroscopy is not exploited in clinical practice, because nearly all these studies were trial

of concept studies [18]. The progression of medical diagnosis based on vibrational spectroscopy involves two-phase project: the first one is diagnosis or classification of biomarkers and the second one is identification of the collected biomarkers [19]. FTIR spectra allow for identification of the wide biochemical alterations induced by disease via the acquired metabolic fingerprint from it. Spectral analysis and biomarker identification are required a reduction in the number of spectral variables (wavenumbers) form hundreds to about a dozen, in order to minimize the influence of redundant variables and noise [20]. This can be done by combining principal component analysis (PCA) and Orthogonal Partial Least Squares Discriminant Analysis (OPLS-DA) with FTIR spectral data [21]. The aim of the present work is to evaluate the ability of FTIR spectroscopy to obtain a global metabolic profile useful for the assessment of patients with hypothyroidism (HT). For that, the first part of this study will present a chemo metric analysis approach for discriminating HT patients, while the second part will propose the biochemical assignment of the selected FTIR spectral markers.

Materials and Methods

Study Population and Serum Sample Preparation

The blood samples were collected, using a plain tube. After withdrawal from 26 patients (women) and 26 healthy sex-matched individuals, the blood samples were centrifuged at 3000 rpm for 10 min to collect sera for storage at 40℃. The sera were thawed at room temperature when necessary for the analysis stage. All individuals were fully informed and given the consent forms prior to this study; from each patient, a standard medical history was obtained as well as clinically examined and diagnosed by endocrinologist in the Specialized Center for Endocrinology and Diabetes during November 2018 to July 2019. This study was approved by the Ethics Board of the College of Pharmacy/Mustansiriyah University/Baghdad/Iraq.

Hormonal Assessment

Serum levels of thyroid function including TSH and T4 were estimated by the Enzyme-Linked Fluorescent Assay (ELFA) technique using a commercially available kit (VIDAS® Thyroid panel) from BIOMERIEUX (Lyon, France). All of the assay steps were performed automatically by the MINI VIDAS analyzer from BIOMERIEUX, France. The normal range for TSH was taken as 0.25-5 μU/ml, for T4 it was 60-120 nmol/l. These ranges are in accordance with the available kit.

Analyses were conducted using Microsoft Excel 2010 software. Data were represented as mean±standard deviation. Variables were compared between patient and healthy control groups using Student's t-test. $P<0.05$ was considered statistically significant.

FTIR Spectral Data Acquisition

Infrared spectra were acquired with Fourier transform infrared spectrophotometer (FTIR-8400S, SHIMADZU). Spectra were recorded in absorption mode in the spectral region 400-4000 cm^{-1}, with 45 scans and a resolution of 4 cm^{-1}. During acquisition, room temperature and humidity were maintained at 23℃ and ±39% respectively. After thawing the frozen liquid samples, 10 μl of a liquid sample (serum) was spread on a 3 cm diameter of KBr cell. To avoid the interference of the previously analyzed samples, KBr cell was cleaned using Chloroform (stab/Amylene) HPLC (Biosolve; cat no. 03080602) between each sample. The measurements were performed in a triplicate for each liquid serum sample.

FTIR Spectral Pre-Treatment

First, the dimensionalities of the spectra were reduced to three specific biochemical component regions 900-1200 cm^{-1}, 1500-1700 cm^{-1} and 2800-3100 cm^{-1} dominated by the spectral features of carbohydrates and nucleic acids, proteins (amide I and amide II) and lipids absorption, respectively. Subsequently, second derivatives were calculated, smoothed using a 13-point Savitzky-Golay algorithm. Finally, the spectra were normalized by vector normalization over the whole spectral region before converting them into ASCII format and then collected as a single table of Microsoft Excel (2010). The raw FTIR spectral dataset was recorded and pre-processed using Shimadzu IR solution 1.60 software.

Chemometric Analysis of FTIR Spectra and Univariate Statistics

The normalized second derivative FTIR spectral dataset of patient and healthy control groups were averaged and imported into SIMCA 14.1 software (MKS Umetrics AB, Umeå, Sweden) for performing unsupervised principal component analysis (PCA) to qualify and check the homogeneity of data visually as well as to discover and remove the outliers among the samples which might not fit the model, and supervised Orthogonal Partial Least Squares Discriminant Analysis (OPLS-DA) pattern recognition technique to discriminate between these two groups in a scaling parameter of unit variance (UV). The used model was described by the criterion of R2, which reflect the goodness of fit, and Q2, which reflect the goodness of prediction. The variable importance in the projection (VIP) values exceeding 1.5 were selected as the most important peak signal of absorbance for predicted variables in the scatter plots. Furthermore, the significance of each created OPLS-DA model was validated by P-value ($P<0.05$) of CV-ANOVA. Univariate analysis (Student's t-test) between patient with hypothyroidism and healthy control groups was performed (with $p<0.05$) using Microsoft Excel 2010.

Results

Patient and Healthy Population

Overall fifty-two participants were recruited, 26 patients with hypothyroidism and 26 healthy individuals. The clinical and biochemical characteristics of the studied population are summarized in Table 1. All patients and healthy individuals were female. The mean age of the patients was 43.5±10.4 years and the mean age of the healthy individuals was 30.6±10.0 years. There was a statistically significant increase in mean BMI ($p<0.01$) and TSH level ($P<0.01$) and a decrease in mean T4 level ($P<0.01$) was recorded in a hypothyroidism group as compared to control group.

FTIR Spectral Description

To better characterize individual spectral components, second derivative spectra with 13 smoothing points Savitzky-Golay algorithm for the serum FTIR spectra of hypothyroidism and healthy control

Table 1: Clinical and biochemical characteristics of patients with hypothyroidism and control individuals.

Characteristics	Hypothyroidism (n=26) Mean±SD	Control (n=26) Mean±SD	P-value
Age (years)	43.5±10.4	30.6±10.0	$1.67x10^{-5}$
BMI	33.00±6.0	26.36±4.38	$1.85x10^{-4}$
TSH (μU/ml)	6.40±0.9	2.12±0.83	$6.78x10^{-14}$
T4 (nmol/l)	55±15.2	106±18.17	$1.33x10^{-14}$

were normalized, averaged and presented in figure 1. At first glance, the preliminary data demonstrated that the mean FTIR spectra of the hypothyroidism (HT) serum samples (blue lines) were unique when they compared with the healthy control serum samples (red lines), especially the spectrum within the spectral range of carbohydrates and nucleic acids (900-1200 cm^{-1}) and lipids (2800-3100 cm^{-1}), indicative of the metabolic, genomic, and lipidomic variation between hypothyroidism and healthy control individuals.

FTIR Spectral Classification and Biochemical Assignment of the Spectral Signature

The biochemical features from biological samples are extremely complex and, therefore, FTIR data must be analyzed by methods of multivariate analysis. In this study, for a clear assessment of spectral variance over the studied groups for each region we successfully employed Orthogonal Partial Least Squares Discriminant Analysis (OPLS-DA) method to reveal the discrimination in the FTIR spectral profile between hypothyroidism and healthy control sera, after applying principal component analysis (PCA). It was found that spectral regions 900-1200 cm^{-1} (carbohydrates and nucleic acids feature), 1500-1700 cm^{-1} (proteins feature) and 2800-3100 cm^{-1} (lipids feature) have important values for discrimination of hypothyroidism sera. These results suggested variations in the mechanisms of carbohydrates and nucleic acids, proteins and lipids between these two groups. These spectral features are discussed in detail below to determine the mechanism of differences and acquire further insight into the pathophysiological processes of the hypothyroidism. Beside its classification capacities, the OPLS-DA model gives the opportunity to highlight variables that are highly relevant to this discrimination. Univariate analysis (t-test) with $P<0.05$ focused on the variable importance in projection (VIP>1.5) obtained from the OPLS-DA model.

Carbohydrates and Nucleic Acids Region

Unsupervised method (PCA) for 900-1200 cm^{-1} region (carbohydrates and nucleic acids feature) is first achieved to build up a picture of sample variances and determine the outlier sample, from which no outlier samples from both hypothyroidism and healthy control groups falling outside the 95% confidence level of Hotelling's T2 ellipse (Figure 2A). The PCA result presented as score plot of the first two PCs (PC1 (24.1%) and PC2 (18.3)) and the model demonstrated the

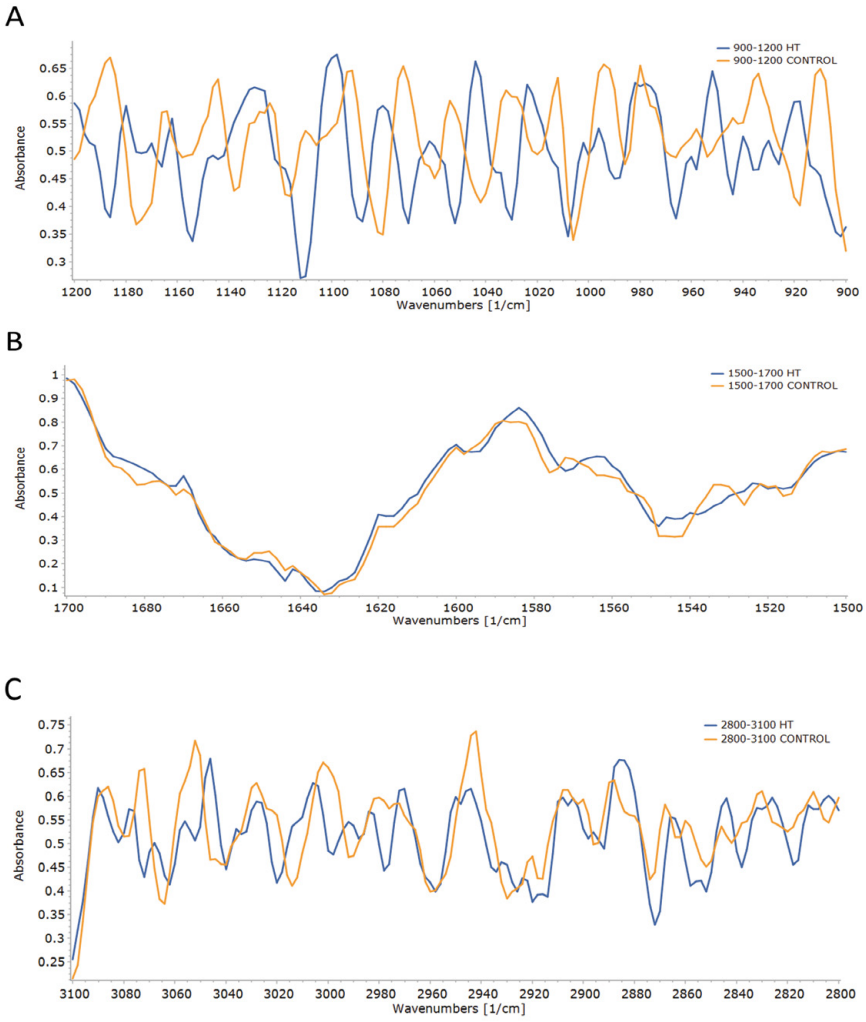

Figure 1: Mean of the normalized second derivative FTIR spectra within the analysis regions obtained from 3 replicates of 26 serum samples for each hypothyroidism (HT) and healthy control group)

(A) 900-1200 cm^{-1} region (B) 1500-1700 cm^{-1} region and (C) 2800-3100 cm^{-1} region. X-axes represent the wavenumber (cm^{-1}) and Y-axes represent the absorbance. Blue color lines correspond to patients with hypothyroidism (HT) and red color lines correspond to healthy control groups.

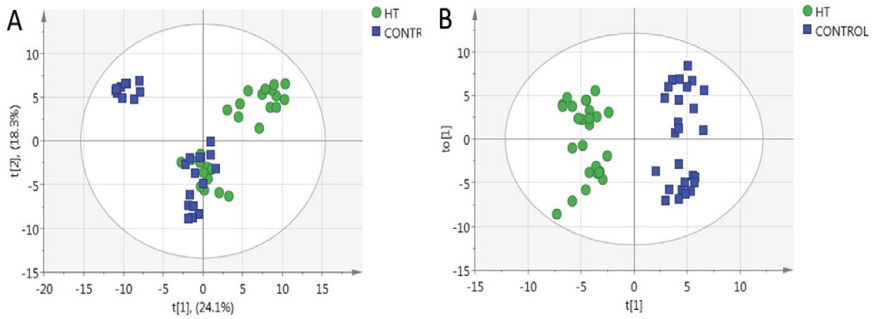

Figure 2: PCA and OPLS-DA Score plots of carbohydrates and nucleic acids region. (A) Principal component analysis (PCA) score plot of second derivative FTIR spectra, with component 1 (X-axis) showing 24.1% and component 2 (Y-axis) showing 18.3% of the variation, and (B) The corresponding OPLS-DA score plot, X-axis indicates the first principal component and Y-axis indicates the first orthogonal component.

Table 2: Possible FTIR band assignments of variables with the highest discriminatory power of the hypothyroidism (HT) and healthy control groups in the carbohydrate and nucleic acid (900-1200 cm^{-1}) spectral region.

Wave number (cm^{-1})	Absorbance		P value	VIP value	Literature Assignment
	Hypothyroidism	Control			
1092	0.420678	0.645973	$2.16x10^{-8}$	1.60906	Symmetric stretching vibration of PO_2^- of DNA [22]
1080	0.581613	0.348844	$8.1x10^{-10}$	1.5563	Symmetric stretching vibration of nucleic acid [23] C-O symmetric stretching of glucose [24]
1112	0.270342	0.516188	$5.05x10^{-9}$	1.55226	Glycogen band [25] Symmetric of phosphate [26]
1082	0.574111	0.354344	$6.66x10^{-8}$	1.54648	Symmetric stretching vibration of PO_2^- of nucleic acid [27] Collagen [28] Glucose [29]

goodness of fit, R2X (cum)=0.782, and predictability, Q2(cum)=0.534. Then, a definitive PCA model is used for a supervised method, OPLS-DA, for the identification of samples.

In the OPLS-DA model, all spectral dataset lay inside the 95% confidence region (Hotelling T2 ellipse) (Figure 2B) of the score plot. The score plot shows a distinct separation between hypothyroidism and healthy control groups, and the samples distributed in each group's region. OPLS-DA model shows a good fit with R2Y=0.934 and predictability with Q2=0.514; validation of the model for predictive ability was assessed with significant (P<0.05) cross validated–ANOVA (CV-ANOVA). These findings suggested variations in the pathophysiological processes of the hypothyroidism.

Ellipses represent the 95% confidence intervals. Circles represent hypothyroidism (HT) group (n=26), squares represent healthy control group (n=26). The differential variables (wave numbers) were selected using the criteria with both variable importance in projection (VIP) value over 1.5 in OPLS-DA model and p<0.05 according to Student's t-test. Table 2 represents the main assignments of an apparent change in the absorption of the selected variables (wavenumbers) in the region (900-1200 cm^{-1}), that predominated by the vibration of PO_2^- of nucleic acid, C-O vibration of glucose, glycogen, collagen and glucose at different wavenumbers including 1092, 1080, 1112, and 1082 cm^{-1}.

Proteins Region

Unsupervised method (PCA) for 1500-1700 cm^{-1} region (proteins feature) is first achieved to build up a picture of sample variances and determine the outlier sample, from which two outlier samples from healthy control group falling outside the 95% confidence level of Hoteling's T2 ellipse (Figure 3A). The result presented as score plot of the first two PCs (PC1 (36.1%) and PC2 (20.7%)) of this PCA model and demonstrated the goodness of fit, R2X (cum)=0.983, and predictability, Q2 (cum)=0.848. Then, a definitive PCA model is used for a supervised method, OPLS-DA, for the identification of samples. In the OPLS-DA model, all spectral dataset lay inside the 95% confidence region (Hotelling T2 ellipse) (Figure 3B) of the score plot. The score plot shows definite hypothyroidism and healthy control grouping with a small overlap after excluding two outlier samples from the healthy control group. OPLS-DA model shows a good fit with R2Y=0.726 and predictability with Q2=0.555; validation of the model for predictive ability was assessed with significant (P<0.05) cross validated-ANOVA (CV-ANOVA). These findings suggested variations in the pathophysiological processes of the hypothyroidism.

Circles represent hypothyroidism (HT) group (n=26) for PCA and OPLS-DA score plot, squares represent healthy control group (n=26) for PCA and (n=24) for OPLS-DA. The differential variables (wave numbers) were selected using the criteria with both variable importance in projection (VIP) value over 1.5 in OPLS-DA model and p<0.05 according to Student's t-test. Table 3 represents the main assignments of an apparent change in the absorption of the selected variables (wavenumbers) in the region (1500-1700 cm^{-1}), that predominated by the vibration of N-H, C-N, and C=O in amide I and II at different wavenumbers including 1578, 1576, 1580 and 1682 cm^{-1}.

Lipids Region

Unsupervised method (PCA) for 2800-3100 cm^{-1} region (lipids feature) is first achieved to build up a picture of sample variances and determine the outlier sample, from which no outlier sample from both hypothyroidism and healthy control groups falling outside the 95% confidence level of Hotelling's T2 ellipse (Figure 4A). The PCA result presented as score plot of the first two PCs (PC1 (21.3%) and PC2 (15.2)) and the model demonstrated the goodness of fit, R2X(cum)=0.768, and predictability, Q2(cum)=0.389. Then, a definitive PCA model is used for a supervised method, OPLS-DA, for the identification of samples.

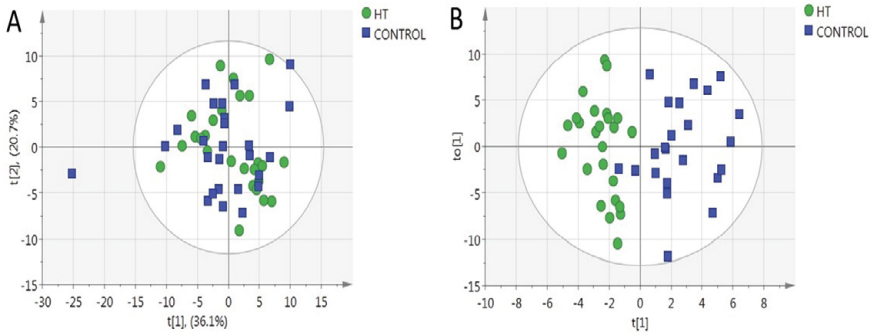

Figure 3: PCA and OPLS-DA Score plots of proteins region. (A) Principal component analysis (PCA) score plot of second derivative FTIR spectra, with component 1 (X-axis) showing 36.1% and component 2 (Y-axis) showing 20.7% of the variation, and (B) The corresponding OPLS-DA score plot, X-axis indicates the first principal component and Y-axis indicates the first orthogonal component. Ellipses represent the 95% confidence intervals.

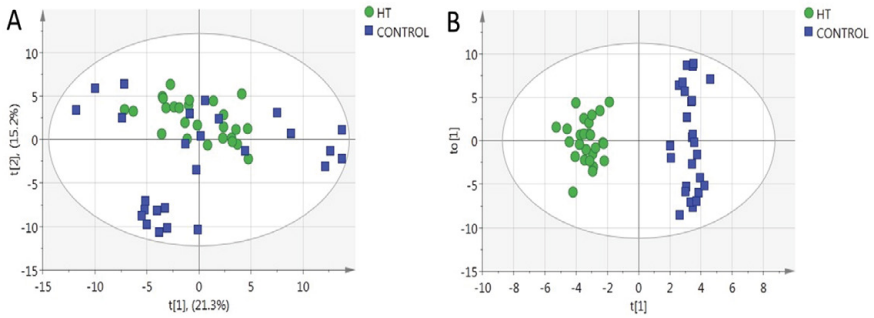

Figure 4: PCA and OPLS-DA Score plots of lipids region: (A) Principal component analysis (PCA) score plot of second derivative FTIR spectra, with component 1 (X-axis) showing 21.3% and component 2 (Y-axis) showing 15.2% of the variation, and (B) The corresponding OPLS-DA score plot, X-axis indicates the first principal component and Y-axis indicates the first orthogonal component. Ellipses represent the 95% confidence intervals.

Table 3: Possible FTIR band assignments of variables with the highest discriminatory power of the hypothyroidism (HT) and healthy control groups in the protein (1500-1700 cm^{-1}) spectral region.

Wavenumber (cm^{-1})	Absorbance		P-value	VIP value	Literature Assignment
	Hypothyroidism	Control			
1578	0.7458	0.6566	$7.53x10^{-6}$	1.87239	N-H bending vibration coupled to C-N stretching vibration (amide II) [30]
1576	0.6748	0.5942	$2.27x10^{-4}$	1.58854	N-H bending vibration coupled to C-N stretching vibration (amide II)
1580	0.7990	0.7397	$4.7x10^{-4}$	1.58277	N-H bending vibration coupled to C-N stretching vibration (amide II)
1682	0.6249	0.5512	$9.69x10^{-4}$	1.52427	C=O stretch vibration coupled to N-H bend vibration (amide I)

In the OPLS-DA model, all spectral dataset lay inside the 95% confidence region (Hotelling T2 ellipse) (Figure 4B) of the score plot. The score plot shows a distinct separation between hypothyroidism and healthy control groups and the samples distributed in each group's region. OPLS-DA model shows a good fit with R2Y=0.959 and predictability with Q2=0.618; validation of the model for predictive ability was assessed with significant ($P<0.05$) cross validated–ANOVA (CV-ANOVA). These findings suggested variations in the pathophysiological processes of the hypothyroidism.

Circles represent hypothyroidism (HT) group (n=26), squares represent healthy control group (n=26). The differential variables (wave numbers) were selected using the criteria with both variable importance in projection (VIP) value over 1.5 in OPLS-DA model and $p<0.05$ according to Student's t-test. Table 4 represents the main assignments of an apparent change in the absorption of the selected variables (wavenumbers) in the region (2800-3100 cm^{-1}), that predominated by the vibration of C-H ring, CH_3, C-H, =CH, and CH_2 at different wavenumbers including 3072, 2870, 3074, 2998, 3052, 3000, 2978, 3020, 3050, and 2858 cm^{-1}.

Discussion

In this study, we have tried to explore the use of FTIR spectroscopy coupled with chemo metric analysis in the detection of potential biomarkers in the serum of hypothyroidism and the possibility of this methodology serving as a complementary tool for Nuclear Magnetic Resonance (NMR) and Mass Spectrometry (MS). To our knowledge, the first application of FTIR to human hypothyroidism sera is presented here. The presented data (OPLS-DA results) described above show that FTIR-based metabolic profiling can discriminate and recognize functional groups that exist in metabolites. These metabolites were found in the carbohydrates and nucleic acids (900-1200 cm^{-1}), proteins (1500-1700 cm^{-1}), and lipids (2800-3100 cm^{-1}) absorption regions. Suggesting that irregularities in the metabolic pathways involving these biomolecules have been associated with the change of adverse

Table 4: Possible FTIR band assignments of variables with the highest discriminatory power of the hypothyroidism (HT) and healthy control groups in the lipid (2800-3100 cm^{-1}) spectral region.

Wavenumber (cm^{-1})	Absorbance		P-value	VIP value	Literature Assignment
	Hypothyroidism	Control			
3072	0.4292	0.6570	$1.86x10^{-6}$	1.92344	C-H ring [31]
2870	0.3563	0.5296	$4.20x10^{-6}$	1.914	CH_3 symmetric stretching of lipid [32]
3074	0.4643	0.6532	$8.80x10^{-7}$	1.86943	C-H ring [31]
2998	0.4769	0.6419	$2.22x10^{-6}$	1.74388	C-H stretching of lipid [33]
3052	0.5064	0.7173	$1.07x10^{-5}$	1.68639	C-H Symmetric stretching of methyl group [34]
3000	0.4849	0.6597	$1.16x10^{-6}$	1.67162	Olefinic=CH [35,36]
2978	0.4434	0.5901	$7.47x10^{-5}$	1.56612	C-H stretching of lipid [33,35]
3020	0.4179	0.5607	$1.46x10^{-4}$	1.55766	Olefinic=CH stretch (unsaturated lipid) [30,36]
3050	0.5347	0.6863	$3.77x10^{-4}$	1.52942	C-H stretching of aromatic [37]
2858	0.4104	0.5358	$3.86x10^{-4}$	1.51192	CH_2 Symmetric stretching vibration [38,39]

metabolic effects in patients with hypothyroidism [40,41]. Thyroid hormone has been known to control various metabolic processes essential for regulating metabolism in the human body [40,41]. It has been documented that thyroid hormone regulates the metabolism of carbohydrates via gluconeogenesis and glycogenolysis pathways [42,43], proteins via protein catabolizing lysosomal enzymes [44], and lipids via the oxidation of fatty acids and cholesterol metabolism [45]. The sensitivity of FTIR spectroscopy is very high for carbohydrates, lipids, proteins, and nucleic acids vibration. The absorbance of infrared in the first spectral region (complicated region) at 900-1200 cm^{-1} is attributed to the presence of carbohydrates, phosphates and nucleic acids vibration and absorption [46]. According to previous studies by Fabian H, et al. (1995) [47], and Wood BR, et. al. (1998) [48], the spectral region between 1000 and 1150 cm^{-1} is typical for carbohydrate while the region between 900 and 1300 cm^{-1} is predominantly for nucleic acids. The results indicate that the serum absorption of hypothyroidism decreases at 1092 and 1112 cm^{-1}, while increases at the region 1080-1082 cm^{-1}. These changes would give a signature in this region of FTIR spectra that is characteristic of hypothyroidism. However, it has been documented that the absorption of nucleic acids dramatically affect by environmental factors and only reveals clearly in the absence of glycogen [49]. Thus, the variation in nucleic acid signals can be influenced by changes in glycogen and phosphate contents which have overlapping absorbance with nucleic acids in this region and make it difficult to precisely identify and measure the change in any peak wavenumber value during such alterations [50]. Since the absorbance is dependent on the concentration of different biomolecules in the sample, alteration of any biomolecules with respect to each other would distinct themselves as changes in the spectra. These are perhaps the reason for the decreased absorbance at 1092 and 1112 cm^{-1} and increased absorbance in the region 1080-1082 cm^{-1} in the serum of patients with hypothyroidism. Increases in the proteins spectral region (1500-1700 cm^{-1}), the second region, of patients with hypothyroidism at 1576, 1578, 1580, 1682 cm^{-1} suggest an increase in protein content as compared with control individuals. Considering this observed change in the underlying characteristics of the protein region is not possible from this work alone to determine what changes in protein secondary structure or protein folding or unfolding events may have occurred as a result of the disease. The changes in the amide I bands reflect the symmetry of secondary structures, whereas the changes in the amide II bands reflect directly the coupling between hydration water and protein residuals. Our result showed that patients with hypothyroidism altered both the amide I and amide II bands, and thus affected the protein content. Furthermore, the association of low-grade inflammation is known in patients with even mild degrees of hypothyroidism [51]. The resultant increase in serum protein content of patients with hypothyroidism has been reported previously [52,53]. In patients with hypothyroidism decreases were observed in the lipid spectral region (2800-3100 cm^{-1}), the third region, at 2858, 2870, 2978, 2998, 3000, 3020, 3050, 3052, 3072, 3074 cm^{-1} as compared with control individuals suggest a decrease in the lipids content. It was documented that the decreased levels of thyroid hormones decrease serum free fatty acids, however increase cholesterol, and triglyceride levels [54]. The release of free fatty acids from triacylglycerol stores in hepatic cells is mediated by the enzymatic activity of cytosolic lipase [55]. So, the decrease in fatty acids content can occur as a result of a decline in hepatic lipase activity [56] as this enzyme is sensitive to thyroid hormone [57]. Since then, the decreased levels of fatty acids in the serum of patients with hypothyroidism have been reported previously [58]. Furthermore, fatty acid synthesis is regulated by fatty acid synthase gene, which encodes fatty acid synthase enzyme, is down-regulated in the liver of patients with hypothyroidism [59]. This study prove the ability of FTIR spectroscopic approach which, although not giving a definite picture of the different metabolic alteration, solely based on FTIR spectral data and subsequent chemo metric analysis shows satisfactory method of diagnosis.

Conclusion

The FTIR-based spectroscopic technique, which is a simple, cost-effective and high-throughput method, could be used as a powerful technique in a clinical laboratory to discriminate the profiling of patients' serum with hypothyroidism. Combining FTIR spectroscopy with chemo metric analysis provided a method for hypothyroid diagnosis. OPLS-DA analysis of second derivative spectra revealed 18 data-points providing from different spectral regions more discriminatory power to identify the differences and similarities between sera of patients with hypothyroidism and healthy individuals. These peaks showed characteristic patterns in the samples of patients with hypothyroidism and healthy individuals. This combination between vibrational spectroscopy and chemo metric analysis provides understanding serum-based bio-molecule composition at different FTIR absorption regions and could serve as useful tool in clinical diagnosis of hypothyroidism after further validation in depth.

References

1. Brix K, Führer D, Biebermann H (2011) Molecules important for thyroid hormone synthesis and action - known facts and future perspectives. Thyroid Res 4: S1-S9.
2. Kim B (2008) Thyroid hormone as a determinant of energy expenditure and the basal metabolic rate. Thyroid 18: 141-144.
3. Panicker V, Wilson SG, Walsh JP, Richards JB, Brown SJ, et al. (2010) A locus on chromosome 1p36 is associated with thyrotropin and thyroid function as identified by genome-wide association study. Am J Hum Genet 87: 430-435.

4. Moreno M, de Lange P, Lombardi A, Silvestri E, Lanni A, et al. (2008) Metabolic effects of thyroid hormone derivatives. Thyroid 18: 239-253.

5. Pietzner M, Engelmann B, Kacprowski T, Golchert J, Dirk AL, et al. (2017) Plasma proteome and metabolome characterization of an experimental human thyrotoxicosis model. BMC Med 15: 6.

6. Ogbonna SU, Ezeani IU (2019) Risk factors of thyroid dysfunction in patients with type 2 diabetes mellitus. Front Endocrinol 10: 440.

7. Parachalil DR, Bruno C, Bonnier F, Blasco H, Chourpa I, et al. (2019) Analysis of bodily fluids using vibrational spectroscopy: a direct comparison of Raman scattering and infrared absorption techniques for the case of glucose in blood serum. Analyst 144: 3334-3346.

8. Correia M, Lopes J, Silva R, Rosa I, Henriques A, et al. (2016) FTIR spectroscopy - a potential tool to identify metabolic changes in dementia patients. J Alzheimers Neurodegener Dis 2: 1-9.

9. Movasaghi Z, Rehman S, ur Rehman DI (2008) Fourier Transform Infrared (FTIR) Spectroscopy of biological tissues. Appl Spectrosc Rev 43: 134-179.

10. Mitchell AL, Gajjar KB, Theophilou G, Martin FL, Martin-Hirsch PL (2014) Vibrational spectroscopy of biofluids for disease screening or diagnosis: translation from the laboratory to a clinical setting: Vibrational spectroscopy of biofluids: laboratory to clinical setting. J Biophotonics 7: 153-165.

11. Kallenbach-Thieltges A, Großerüschkamp F, Mosig A, Diem M, Tannapfel A, et al. (2013) Immunohistochemistry, histopathology and infrared spectral histopathology of colon cancer tissue sections. J Biophotonics 6: 88-100.

12. Backhaus J, Mueller R, Formanski N, Szlama N, Meerpohl HG, et al. Diagnosis of breast cancer with infrared spectroscopy from serum samples. Vib Spectrosc 52: 173-177.

13. Ollesch J, Heinze M, Heise HM, Behrens T, Brüning T, et al. (2014) It's in your blood: spectral biomarker candidates for urinary bladder cancer from automated FTIR spectroscopy: Spectral cancer biomarkers from high-throughput FTIR spectroscopy. J Biophotonics 7: 210-221.

14. Hands JR, Dorling KM, Abel P, Ashton KM, Brodbelt A, et al. (2014) Attenuated Total Reflection Fourier Transform Infrared (ATR-FTIR) spectral discrimination of brain tumour severity from serum samples: Serum spectroscopy gliomas. J Biophotonics 7: 189-199.

15. Barlev E, Zelig U, Bar O, Segev C, Mordechai S, et al. (2016) A novel method for screening colorectal cancer by infrared spectroscopy of peripheral blood mononuclear cells and plasma. J Gastroenterol 51: 214-221.

16. Peuchant E, Richard-Harston S, Bourdel-Marchasson I, Dartigues JF, Letenneur L, et al. (2008) Infrared spectroscopy: a reagent-free method to distinguish Alzheimer's disease patients from normal-aging subjects. Transl Res 152: 103-112.

17. Travo A, Paya C, Déléris G, Colin J, Mortemousque B, et al. (2014) Potential of FTIR spectroscopy for analysis of tears for diagnosis purposes. Anal Bioanal Chem 406: 2367-2376.

18. Baker MJ, Hussain SR, Lovergne L, Untereiner V, Hughes C, et al. (2016) Developing and understanding biofluid vibrational spectroscopy: a critical review. Chem Soc Rev 45: 1803-1818.

19. Trevisan J, Park J, Angelov PP, Ahmadzai AA, Gajjar K, et al. (2014) Measuring similarity and improving stability in biomarker identification methods applied to Fourier-transform infrared (FTIR) spectroscopy: Stability and similarity in biomarker identification in FTIR spectroscopy. J Biophotonics 7: 254-265.

20. Le Corvec M, Jezequel C, Monbet V, Fatih N, Charpentier F, et al. (2017) Mid-infrared spectroscopy of serum, a promising non-invasive method to assess prognosis in patients with ascites and cirrhosis. PLoS One 12: e0185997.

21. Worley B, Powers R (2016) PCA as a practical indicator of OPLS-DA model reliability. Curr Metabolomics 4: 97-103.

22. Vidal B de C, Ghiraldini FG, Mello MLS (2014) Changes in liver cell DNA methylation status in diabetic mice affect its FT-IR characteristics. PLoS One 9: e102295.

23. Sheng D, Wu Y, Wang X, Huang D, Chen X, et al. (2013) Comparison of serum from gastric cancer patients and from healthy persons using FTIR spectroscopy. Spectrochim Acta A Mol Biomol Spectrosc 116: 365-369.

24. Roy S, Perez-Guaita D, Andrew DW, Richards JS, McNaughton D, et al. (2017) Simultaneous ATR-FTIR based determination of malaria parasitemia, glucose and urea in whole blood dried onto a glass slide. Anal Chem 89: 5238-5245.

25. Wood BR, Kiupel M, McNaughton D (2014) Progress in Fourier transform infrared spectroscopic imaging applied to venereal cancer diagnosis. Vet Pathol 51: 224-237.

26. Argov S, Ramesh J, Salman A, Sinelnikov I, Goldstein J, et al. (2002) Diagnostic potential of Fourier-transform infrared microspectroscopy and advanced computational methods in colon cancer patients. J Biomed Opt 7: 248.

27. Simonova D, Karamancheva I (2013) Application of Fourier transform infrared spectroscopy for tumor diagnosis. Biotechnol Biotechnol Equip 27: 4200-4207.

28. Andrus PGL, Strickland RD (1998) Cancer grading by Fourier transform infrared spectroscopy. Biospectroscopy 4: 37-46.

29. Shen YC, Davies AG, Linfield EH, Elsey TS, Taday PF, et al. (2003) The use of Fourier-transform infrared spectroscopy for the quantitative determination of glucose concentration in whole blood. Phys Med Biol 48: 2023-2032.

30. Malek K, Wood BR, Bambery KR (2014) FTIR imaging of tissues: techniques and methods of analysis. In: Optical Spectroscopy and Computational Methods in Biology and Medicine. Springer, Netherlands.

31. Dovbeshko G (2000) FTIR spectroscopy studies of nucleic acid damage. Talanta 53: 233-246.

32. Wolkers WF, Oldenhof H (2010) In situ FTIR studies on mammalian cells. J Spectrosc 24: 525-534.

33. Perez-Guaita D, Kochan K, Martin M, Andrew DW, Heraud P, et al. (2017) Multimodal vibrational imaging of cells. Vib. Spectrosc 91: 46-58.

34. Vidak A, Šapić IM, Dananić V (2015) Cation-π interaction of N,N-Dimethyltryptamine in hydrochloric acid solution characteristic to gastric acid. Integr Mol Med 2: 354.

35. Cakmak G, Miller LM, Zorlu F, Severcan F (2012) Amifostine, a radioprotectant agent, protects rat brain tissue lipids against ionizing radiation induced damage: An FTIR microspectroscopic imaging study. Arch Biochem Biophys 520: 67-73.

36. HM Ali M, Rakib F, Nischwitz V, Ullah E, Mall R, et al. (2018) Application of FTIR and LA-ICPMS spectroscopies as a possible approach for biochemical analyses of different rat brain regions. Appl Sci 8: 2436.

37. Ketren W, Zen H, Ashida R, Kii T, Ohgaki H (2019) Investigation on conversion pathways in degradative solvent extraction of rice straw by using liquid membrane-FTIR spectroscopy. Energies 12: 528.

38. Igci N, Sharafi P, Ozel Demiralp D, Demiralp C, Yuce A, et al. (2017) Application of Fourier transform infrared spectroscopy to biomolecular profiling of cultured fibroblast cells from Gaucher disease patients: A preliminary investigation. Adv Clin Exp Med 26: 1053-1061.

39. Invernizzi C, Rovetta T, Licchelli M, Malagodi M (2018) Mid and near-infrared reflection spectral database of natural organic materials in the cultural heritage field. Int J Anal Chem 2018: 1-16.

40. Cicatiello AG, Di Girolamo D, Dentice M (2018) Metabolic Effects of the Intracellular Regulation of Thyroid Hormone: Old Players, New Concepts. Front Endocrinol 9: 474.

41. Damiano F, Rochira A, Gnoni A, Siculella L (2017) Action of thyroid hormones, T3 and T2, on hepatic fatty acids: differences in metabolic effects and molecular mechanisms. Int J Mol Sci 18: 744.

42. Brenta G (2011) Why can insulin resistance be a natural consequence of thyroid dysfunction? J Thyroid Res 2011: 1-9.

43. Laville M, Khalfallah Y, Vidai H, Beylot M, Comte B, et al. (1987) Hormonal control of glucose production and pyruvate kinase activity in isolated rat liver cells: influence of hypothyroidism. Mol Cell Endocrinol 50: 247-253.

44. Müller MJ, Seitz HJ (1984) Thyroid hormone action on intermediary metabolism. Part III. Protein metabolism in hyper- and hypothyroidism. Klin Wochenschr 62: 97-102.

45. Gnocchi D, Steffensen KR, Bruscalupi G, Parini P (2016) Emerging role of thyroid hormone metabolites. Acta Physiol 217: 184-216.

46. Lin H, Deng K, Zhang J, Wang L, Zhang Z, et al. (2019) Biochemical detection of fatal hypothermia and hyperthermia in affected rat hypothalamus tissues by Fourier transform infrared spectroscopy. Biosci Rep 39.

47. Fabian H, Jackson M, Murphy L, Watson PH, Fichtner I, et al. (1995) A comparative infrared spectroscopic study of human breast tumors and breast tumor cell xenografts. Biospectroscopy 1: 37-45.

48. Wood BR, Quinn MA, Tait B, Ashdown M, Hislop T, et al. (1998) FTIR microspectroscopic study of cell types and potential confounding variables in screening for cervical malignancies. Biospectroscopy 4: 75-91.

49. Lasch P, Boese M, Pacifico A, Diem M (2002) FT-IR spectroscopic investigations of single cells on the subcellular level. Vib Spectrosc 28: 147-157.

50. Sahu RK, Argov S, Salman A, Huleihel M, Grossman N, et al. (2004) Characteristic absorbance of nucleic acids in the Mid-IR region as possible common biomarkers for diagnosis of malignancy. Technol Cancer Res Treat 3: 629-638.

51. Kvetny J, Heldgaard PE, Bladbjerg EM, Gram J (2004) Subclinical hypothyroidism is associated with a low-grade inflammation, increased triglyceride levels and predicts cardiovascular disease in males below 50 years. Clin Endocrinol 61: 232-238.

52. Arora S, Chawla R, Tayal D, Gupta VK, Sohi JS, et al. (2009) Biochemical markers of liver and kidney function are influenced by thyroid function-a case-controlled follow up study in Indian hypothyroid subjects. Indian J Clin Biochem 24: 370-374.

53. Akhigbe R, Ajayi A (2012) Implication of altered thyroid state on liver function. Thyroid Res Pract 9: 84.

54. Duntas LH, Brenta G (2012) The effect of thyroid disorders on lipid levels and metabolism. Med Clin North Am 96: 269-281.

55. Sinha RA, Singh BK, Yen PM (2018) Direct effects of thyroid hormones on hepatic lipid metabolism. Nat Rev Endocrinol 14: 259-269.

56. Brenta G, Berg G, Miksztowicz V, Lopez G, Lucero D, et al. (2016) Atherogenic lipoproteins in subclinical hypothyroidism and their relationship with hepatic lipase activity: response to replacement treatment with levothyroxine. Thyroid 26: 365-372.

57. Kihara S, Wolle J, Ehnholm C (1993) Regulation of hepatic triglyceride lipase by thyroid hormone in HepG2 cells. J Lipid Res 34: 961-970.

58. Gjedde S, Gormsen LC, Rungby J, Nielsen S, Jørgensen JOL, et al. (2010) Decreased lipid intermediate levels and lipid oxidation rates despite normal lipolysis in patients with hypothyroidism. Thyroid 20: 843-849.

59. Sun J, Sun L, Chen W, Yin X, Lu Y, et al. (2018) A family with hypothyroidism caused by fatty acid synthase and apolipoprotein B receptor mutations. Mol Med Rep 18: 4904-4912.